Magnetic ordering and superconductivity in $Y_{1-x}Pr_xBa_2Cu_3O_{7-y}$

A. Kebede, C. S. Jee, J. Schwegler, J. E. Crow, T. Mihalisin, G. H. Myer, R. E. Salomon, and P. Schlottmann
Center for Materials Research, Temple University, Philadelphia, Pennsylvania 19122

M. V. Kuric, S. H. Bloom, and R. P. Guertin
Physcis Department, Tufts University, Medford, Massachusetts 02155
(Received 22 March 1989)

An extensive study of magnetic, thermal, transport, and structural properties of the alloy $Y_{1-x}Pr_xBa_2Cu_3O_{7-y}$ is presented. The endpoints of the alloy series are a high-temperature superconductor Y-Ba-Cu-O and an antiferromagnetic semiconductor (Pr-Ba-Cu-O, $T_N=17$ K). The superconducting transition temperature is reduced with increasing Pr concentration following the Abrikosov-Gorkov pair-breaking curve with critical concentration $x_{cr}=0.62$. Alloying also reduces the Néel temperature approximately linearly with the Y content, and there is a concentration region ($0.4<x<0.6$) where antiferromagnetism and superconductivity is suggested to coexist. The specific heat, the susceptibility, the magnetic ordering, and the metal-to-semiconductor transition seen in the resistivity are consistent with the picture that Y^{3+} is replaced by Pr^{4+} with some degree of valence admixture of the Pr^{3+} configuration.

I. INTRODUCTION

It was found very early during the "high-T_c" era that most magnetic rare-earth-element substitutions for Y in the 90 K superconductor $YBa_2Cu_3O_{7-y}$ left the superconducting properties essentially unchanged,[1] in strong contrast to the case of conventional superconductors, where the localized magnetic moments associated with the magnetic rare-earth elements are extremely deleterious to the superconducting state.[2] In a conventional superconductor, exchange scattering of conduction electrons by the magnetic moments and the resulting breaking of Cooper pairs, called pair breaking, causes a rapid depression of superconductivity. The insensitivity of the superconducting properties of $YBa_2Cu_3O_7$ to substitution of most of the rare earths for Y is presumably due to the fact that the superconducting electrons are in the CuO planes and do not experience spin-flip scattering off of the moments which substitute on the Y sites located midway between the Cu-O planes. Among the magnetic rare-earth systems that are based on $YBa_2Cu_3O_{7-y}$, Pr-doped $YBa_2Cu_3O_{7-y}$ and the isomorphic compound $PrBa_2Cu_3O_{7-y}$ stand out as anomalous.[3] Pr doping suppresses the superconductivity of $YBa_2Cu_3O_{7-y}$ not unlike the effect of magnetic impurities in conventional superconductors.[4] Moreover, the temperature dependence of the electrical resistivity and the pressure dependence of the superconducting transition temperature, T_c, of Pr-doped $YBa_2Cu_3O_{7-y}$ behave anomalously.[5] Although crystallographically identical to all the other rare-earth-based superconductors, $PrBa_2Cu_3O_{7-y}$ is a semiconductor, with very large electrical resistivity (10^7 Ω cm) at helium temperatures. Tb- and Ce-based analogues may behave similarly, but these have not been fabricated in an isomorphic structure to $YBa_2Cu_3O_{7-y}$.[6] If Pr is trivalent, it is not easy to understand why the substitution of Pr for Y in the 90 K superconductor should have such a profound negative effect on the superconductivity, while other rare earths with local magnetic moments do not. With few exceptions (a few mixed valent and Kondo systems) the properties of most Pr-based alloys and compounds are well behaved, i.e., their magnetic properties can be understood reasonably well from the point of view of localized magnetism if crystal-field effects are taken into account. Generally, the properties of Pr-based compounds and alloys are similar to those of the heavy rare-earth systems when local perturbative effects on the Pr^{3+} orbital angular momentum are taken into account.[7]

In an effort to understand the unique superconducting pair-breaking properties of Pr substituted $YBa_2Cu_3O_{7-y}$ and the unusual magnetic properties of $PrBa_2Cu_3O_{7-y}$, we have undertaken a study of the superconducting and magnetic properties of $(Y_{1-x}Pr_x)Ba_2Cu_3O_{7-y}$, spanning the complete composition range, $0\le x\le 1.0$, i.e., from a 90-K superconductor ($x=0$) to a high-resistivity semiconductor with antiferromagnetism ($x=1.0$).[8] A further motivation for this study is that through an understanding of the pair-breaking interactions associated with Pr substitution for Y, light may be shed on the pairing mechanisms associated with $YBa_2Cu_3O_{7-y}$, and perhaps high-T_c oxide-based superconductors in general. Our study reveals a smooth evolution[3-5,9] of $(Y_{1-x}Pr_x)Ba_2Cu_3O_{7-y}$ from superconductivity ($x<0.6$) to antiferromagnetic ordering ($0.4<x<1.0$) and suggests a magnetic order–superconductivity overlap region for $0.4<x<0.6$. The data indicate that f electrons contributed by the Pr ions play a crucial role in the superconducting pair breaking for Y-rich samples and in the magnetic ordering in Pr-rich samples.

In order to summarize the results of this work, we

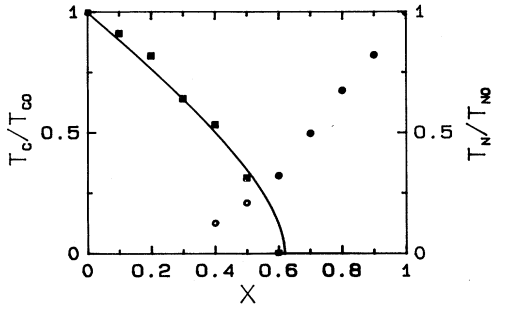

FIG. 1. Superconducting transition temperature T_c and Néel temperature T_N vs Pr concentration in $Y_{1-x}Pr_xBa_2Cu_3O_{7-y}$ with $y \approx 0.1$. T_c and T_N have been normalized to $T_c = 92$ K for $x = 0.0$ and $T_N = 17$ K for $x = 1.0$.

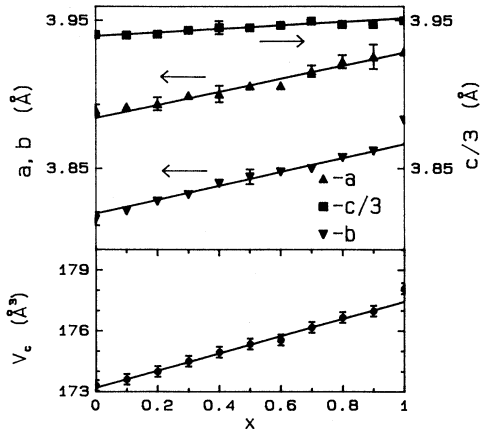

FIG. 2. Orthorhombic lattice constants and unit-cell volume vs Pr concentration in $Y_{1-x}Pr_xBa_2Cu_3O_{7-y}$ for $y \approx 0.1$.

present the entire superconducting-normal phase diagram for $(Y_{1-x}Pr_x)Ba_2Cu_3O_{7-y}$ in Fig. 1. The data are normalized to the transition temperatures of the end members, $T_c = 90$ K for $x = 0$ and $T_N = 17$ K for $x = 1.0$. Note the monotonic decrease in T_c and the rise of magnetic ordering transition temperatures as x increases as well as the region of possible overlap, $0.4 < x < 0.6$.

In Sec. II of this paper we describe the method of preparation of the samples that preserves the orthorhombic $YBa_2Cu_3O_{7-y}$ structure for all compositions, detailed x-ray analysis of all materials, and some experimental details. In Sec. III we focus on the magnetic ordering of $PrBa_2Cu_3O_{7-y}$, and in Sec. IV this analysis is extended to the remaining $(Y_{1-x}Pr_x)Ba_2O_3O_{7-y}$ compositions, $0 < x < 1.0$. A discussion of the results is contained in Sec. V.

II. SAMPLE PREPARATION AND ANALYSIS

Polycrystalline samples of $(Y_{1-x}Pr_x)Ba_2Cu_3O_{7-y}$ for $0.0 \leq x \leq 1.0$ were prepared using a conventional solid-state reaction technique. Stoichiometric quantities of high-purity $BaCO_3$ (99.997%), Y_2O_3 (99.99%), Pr_6O_{11} (99.99%), and CuO (99.999%) were mixed and pressed into pellets using a tungsten carbide pellet press. For $x \leq 0.5$, the nonreacted pellets were calcined at 950 °C for 24 h. The reacted samples were powdered, repressed into pellets, and heated in air at 950 °C for 24 h. This process was repeated three times. These pellets were then heated in flowing oxygen at 950 °C for 12 h, followed by an additional anneal at 500 °C for 12 h. Finally the samples were slowly cooled over several hours to room temperature. For $x > 0.5$, this same procedure was used except the calcining process and the repeated heating to promote homogeneity were limited to 900 °C rather than 950 °C. This lower calcination and processing temperature was necessary to prevent the formation of $PrBa_2O_7$ and other second phases which tend to form for large x at temperatures above 900 °C. Samples were stored in dry oxygen to help prevent deterioration of the samples due to absorption of water and carbon dioxide.

Powder x-ray diffraction studies using a Rigaku automated diffractometer indicated that the samples crystallized in an orthorhombic $YBa_2Cu_3O_{7-y}$ structure for all x. All the samples were essentially single phase with less than 2% impurity phases in most of the samples and less than 3% in all samples. There was no correlation between the Pr content and the amount of second phase present. Both ionic size and valence of Pr^{3+} and Pr^{4+} favors Pr going into the Y site. Thus we believe that the Pr substitutes on the Y site, which is located midway between the Cu-O planes.

Thermal gravimetric analysis was conducted on all samples, and these studies showed that the oxygen loss upon heating to 900 °C in a vacuum or flowing helium was independent of Pr concentration. Based on these measurements and other studies, it appears that the oxygen content is essentially independent of Pr concentration and $y \sim 0.05$–0.10 for all x in $(Y_{1-x}Pr_x)Ba_2Cu_3O_{7-y}$.

We show in Fig. 2 the Pr-concentration dependence of the orthorhombic lattice constants a, b, and c, and the cell volume, V_c. A tabulated summary of the lattice constants for $(Y_{1-x}Pr_x)Ba_2Cu_3O_{7-y}$ with $y \sim 0.1$ is shown in Table I. The system remains orthorhombic for all x with a slight decrease in the orthorhombicity with increasing x. The lattice constants for the fully oxygenated $YBa_2Cu_3O_{7-y}$ are consistent with other published results.[10] All three individual lattice constants increase linearly with x for $0 < x < 1.0$, except b which shows a slightly larger value for $x = 1.0$ than obtained by a linear extrapolation of b versus x from samples with $x \leq 0.9$. This slightly larger value of b for $x = 1.0$ is also reflected in the x dependence of the cell volume. The linear dependence of the lattice constants and cell volume indicate that the Pr valence is not strongly dependent on Pr content.

Shown in Fig. 3 are V_c versus rare-earth ionic radius, r, for $RBa_2Cu_3O_{7-y}$, where R represents Y and all the rare earths except La, Ce, Pm, and Tb. The values of V_c and r are from Refs. 11 and 12, respectively. Also shown in Fig. 3 are two data points indicated as triangles, one for the ionic radius of each valence state of Pr. These points are associated with the measured V_c for $PrBa_2Cu_3O_{7-y}$

TABLE I. Lattice constants and cell volume vs x for $(Y_{1-x}Pr_x)Ba_2Cu_3O_{7-y}$ with $y \sim 0.1$.

x	a (Å)	b (Å)	c (Å)	V (Å^3)
0.0	3.886(7)	3.819(8)	11.678(13)	173.3
0.1	3.888(5)	3.824(4)	11.677(6)	173.6
0.2	3.890(8)	3.830(4)	11.679(11)	174.0
0.3	3.895(4)	3.834(4)	11.686(11)	174.5
0.4	3.896(10)	3.841(6)	11.691(22)	175.0
0.5	3.901(6)	3.845(9)	11.691(8)	175.4
0.6	3.901(4)	3.848(6)	11.695(6)	175.6
0.7	3.910(7)	3.850(5)	11.703(8)	176.2
0.8	3.916(8)	3.857(6)	11.697(7)	176.7
0.9	3.919(15)	3.861(5)	11.697(8)	177.0
1.0	3.922(5)	3.880(6)	11.704(7)	178.1

(including a 2% adjustment to V_c to force our measured value of V_c for $YBa_2Cu_3O_{7-y}$ equal to that in Ref. 11). If the Pr ion were trivalent, V_c for $PrBa_2Cu_3O_{7-y}$ would fall directly on the solid line in Fig. 3. Such a correlation, however, belies the lack of superconductivity in $PrBa_2Cu_3O_{7-y}$ and the accompanying modifications in the normal-state properties, compared to all the other trivalent $RBa_2Cu_3O_{7-y}$ systems. The weight of evidence of this and other published work[3–5,8,9] is that Pr in the $YBa_2Cu_3O_{7-y}$ structure is mixed valent. Therefore, the other point (second triangle) in Fig. 3 which is associated with the tetravalent state of Pr is most appropriate for this system. If one could form other $RBa_2Cu_3O_{7-y}$ systems with tetravalent R's a second straight line parallel to the trivalent one would be present in Fig. 3, which presumably would pass through this point.

All the measurements reported in this paper were performed using fairly standard techniques. The electrical resistivity was measured on rectangular bars cut from the pressed pellets using a standard dc four-probe technique. The specific heat was measured from 1.2 to 25 K using a quasiadiabatic method. For a few samples, the quasiadiabatic measurements of the specific heat were extended to 200 K. For $1.8 \leq T \leq 400$ K and $0 \leq H \leq 5.5$ T, the magnetization and susceptibility were measured using a Quantum Design superconducting quantum interference device (SQUID) magnetometer, and for $2 \leq T \leq 300$ K and $0 \leq H \leq 9$ T, using a vibrating sample magnetometer. Measurements of the magnetization versus magnetic field were extended to 20 T at $T = 4.2$ K for a few samples using the facilities of the Francis Bitter National Magnet Laboratory, MIT.

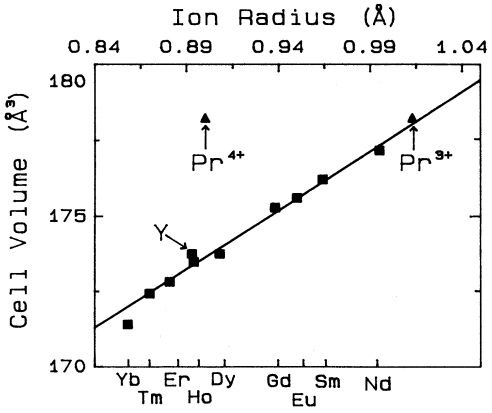

FIG. 3. Cell volume vs ionic radii for $RBa_2Cu_3O_{7-y}$ with R = Y and other rare earths except Ce, Pm, and Tb.

III. MAGNETIC ORDERING OF $PrBa_2Cu_3O_7$

The first evidence for cooperative magnetic ordering in the anomalous nonsuperconducting compound $PrBa_2Cu_3O_{7-y}$ was the discovery of a maximum in the temperature dependence of the heat capacity $C(T)$, at about $T = 17$ K.[8] The $C(T)$ data of $PrBa_2Cu_3O_{7-y}$ for $2 \leq T \leq 20$ K are shown in Fig. 4(a), where this maximum is clearly seen. The $C(T)$ peak near 17 K in Fig. 4(a) is probably too narrow to be associated with a conventional

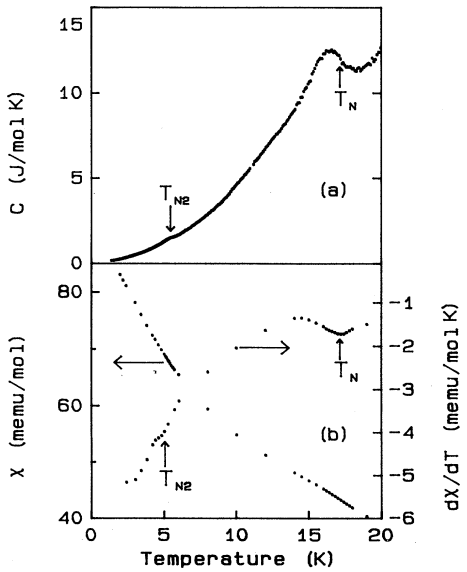

FIG. 4. The specific heat $C(T)$, magnetic susceptibility $\chi(T)$, and temperature derivative of magnetic susceptibility $d\chi/dT$ vs temperature for $PrBa_2Cu_3O_{7-y}$ with $y \approx 0.1$. T_N and T_{N2} mark anomalies in $C(T)$ and $\chi(T)$.

Schottky anomaly, which might arise through thermal depopulation of low-lying Pr-associated crystal-field excitations. Preliminary inelastic neutron scattering data on $PrBa_2Cu_3O_{7-y}$ does not show any excitations in this energy range that could be associated with crystalline electric fields (CEF) excitations.[13] In addition to the rather sharp maximum at around 17 K there is a much smaller feature in $C(T)$ versus T at about 5 K (labeled T_{N2}).[8] In Fig. 4(b), we show the magnetic susceptibility, $\chi(T)$ (taken at 0.1 T) of $PrBa_2Cu_3O_{7-y}$ over the same temperature region, along with $d\chi/dT$ versus T. Both the 17-K and 5-K anomalies show up readily in the $d\chi/dT$ data. The continuing increase of $\chi(T)$ *below* 17 K is at variance with conventional antiferromagnetic order. The magnetic susceptibility versus temperature of $PrBa_2Cu_3O_{7-y}$ and $Y_{0.2}Pr_{0.8}Ba_2Cu_3O_{7-y}$ was also measured in several high fields up to 9 T. Shown in Fig. 5 is $\chi(T)$ and $d\chi(T)/dT$ versus T for $PrBa_2Cu_3O_{7-y}$ with $y \approx 0.1$ and measured in $H=1$, 3, and 5 T. This data was taken on an aligned powder sample, where the powder was introduced into epoxy and allowed to harden in a magnetic field of 15 T.[14] An accurate estimate of the degree of alignment for this sample has not been determined but a very high level of c axis alignment was apparent in x-ray analysis. Note, there is about a factor of 2 anisotropy in $\chi(T)$ versus T with $H \| c$ and $H \perp c$. Shown in the lower portion of Fig. 5 is $d\chi/dT$ versus T for $PrBa_2Cu_3O_{7-y}$. Applying large magnetic fields caused no discernible change in the temperature of the $\chi(T)$ anomaly near 17 K, i.e., the position of the anomaly is field independent up to 9 T. At 9 T we obtain $T_N = 16.9 \pm 0.1$ K. The independence of T_N for $PrBa_2Cu_3O_{7-y}$ is dramatically shown in Fig. 6, where T_N for $PrBa_2Cu_3O_{7-y}$ and $GdBa_2Cu_3O_{7-y}$ (Ref. 15) with $y \approx 0.1$ versus H are compared. This argues against conventional antiferromagnetism, where a field of a few tesla might be expected to suppress T_N by a few degrees Kelvin. Also, any field-dependent anomalies, for example a spin-flop transition,

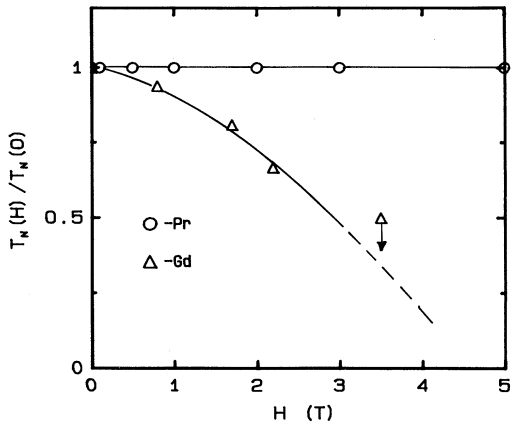

FIG. 6. The Néel temperature vs applied magnetic field for $PrBa_2Cu_3O_{7-y}$ and $GdBa_2Cu_3O_{7-y}$ with $y \approx 0.1$. ($GdBa_2Cu_3O_{7-y}$ data from Ref. 15.)

associated with the 17 K transition must be at fields higher than 9 T. Conventional ferromagnetic order in $PrBa_2Cu_3O_{7-y}$ and other Pr-rich materials showing magnetic anomalies is unlikely, not only because the transition temperature is independent of applied field, but also because no magnetic hysteresis could be detected using sensitive low-field magnetometry at $T \ll 17$ K. Furthermore, for $PrBa_2Cu_3O_7$ conventional ferromagnetism is excluded by neutron studies (see Ref. 16 as well as further discussion).

In Fig. 7 we show the $T=4.2$ K isothermal magnetization, $M(H)$, of $PrBa_2Cu_3O_{7-y}$, taken in fields up to 20 T. As already indicated, no magnetic hysteresis was detected using sensitive low-field magnetometry down to 1.5 K. Note that $M(H)$ never reaches saturation, even at 20 T. The largest value of M reached at 20 T is only 38% of the Pr^{3+} saturation moment and 57% of the Pr^{4+} saturation moment. There is a reasonably pronounced negative cur-

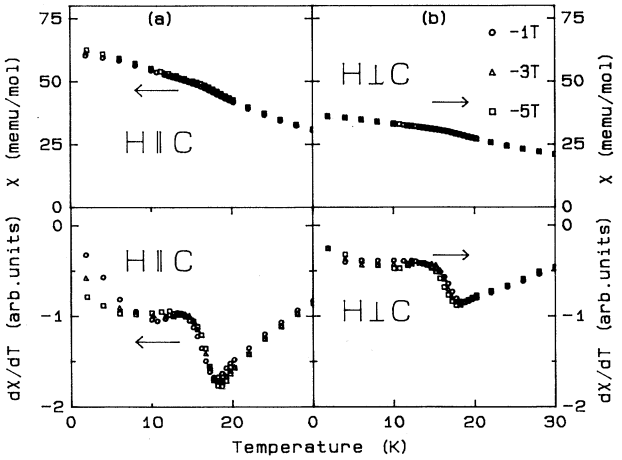

FIG. 5. The magnetic susceptibility $\chi(T)$ and the temperature derivative of the magnetic susceptibility, $d\chi/dT$ vs temperature in $H=1$, 3, and 5 T for a partially aligned powder sample of $PrBa_2Cu_3O_{7-y}$ with $y \approx 0.1$.

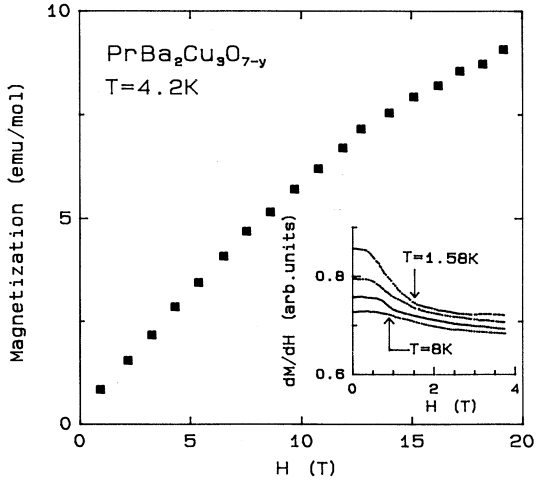

FIG. 7. Isothermal magnetization for $PrBa_2Cu_3O_{7-y}$ vs magnetic field H at $T=4.2$ K. Inset: Magnetic field derivative of the isothermal magnetization dM/dH vs magnetic field.

vature in $M(H)$ at about 1 T for $T<17$ K suggesting weak ferromagnetic order, but this contention is not supported by other experimental evidence.[16] The inset of Fig. 7 shows derivatives of M versus H for several temperatures, bracketing the temperature associated with the lower (5 K) transition-like feature seen in the $C(T)$ and $d\chi/dT$ data. The increase in dM/dH for $T<5$ K and for $H<0.5$ T is taken as evidence for additional magnetic ordering below this temperature. However, aside from these features, no microscopic evidence supports this, and the possibility of an impurity phase cannot be ruled out.

The magnetic ordering of $PrBa_2Cu_3O_{7-y}$ at 17 K is unusual from several points of view. First the ordering temperature is much higher, perhaps by 2 orders of magnitude, than the value extrapolated from the ordering of the other $RBa_2Cu_3O_{7-y}$ antiferromagnets. For example, $T_N=2.2$ K for the isomorphic rare-earth compound $GdBa_2Cu_3O_{7-y}$.[17] The spin angular momentum associated with the Gd moment is $\frac{7}{2}$, and if we estimate the other rare-earth ordering temperatures based on this value by scaling with the de Gennes factor, $g^2J(J+1)$ (where g is the Lande factor and J is the total angular momentum), we estimate magnetic ordering for $PrBa_2Cu_3O_{7-y}$ should occur at about 0.2 K for either of the possible integral Pr-ion configurations, Pr^{3+} ($J=4$) or Pr^{4+} ($J=\frac{5}{2}$). Of course, a dipolar interaction cannot account for a T_N of 17 K. The "de Gennes factor" scaling estimate is independent of the nature of the exchange interaction but assumes the same interaction type and strength for all members of the series. In that case the ordering temperature depends only on the angular momentum state of the rare-earth ion. If crystal-field effects are invoked to partially lift the $2J+1$ degeneracy of the spin-orbit ground state for Pr^{3+} or Pr^{4+}, the ordering temperature for $PrBa_2Cu_3O_{7-y}$ would be reduced even further, particularly for the trivalent state, where a crystal-field singlet ground state would be expected, and only ordering via van Vleck magnetism would be possible. Secondly, as pointed out previously, the susceptibility of $PrBa_2Cu_3O_{7-y}$ increases below the apparent ordering temperature, unlike $\chi(T)$ for conventional antiferromagnetic ordering, where the magnetic susceptibility decreases below T_N. The Gd contribution to the susceptibility for superconducting or oxygen-depleted $GdBa_2Cu_3O_{7-y}$ shows this conventional antiferromagnetic behavior.[15,17] Thirdly, the entropy associated with the ordering is only about 5.0 J/mol K. This is slightly less than the entropy associated with a magnetic doublet ground state, i.e., 5.7 J/mol K. For the Pr^{4+} configuration one expects to find a doubled ground state if the crystal field is strong since the Pr ions are at sites of low symmetry. For Pr^{3+}, as stated earlier, the CEF ground state would be a singlet, and if van Vleck–induced transition did occur, the entropy removal due to the transition would be exponentially dependent on the CEF splitting, and would probably lead to a negligibly small entropy change.

These considerations suggest that either the magnetic ordering associated with the 17-K heat capacity and susceptibility anomalies is not entirely three dimensional or that some portion of the magnetic moment does not enter into the ordering. Cooper[18] has discussed magnetic ordering in Pr-rich $(Y_{1-x}Pr_x)Ba_2Cu_3O_{7-y}$ in terms of cooperative valence fluctuations of the Cu ions mediated through hybridization effects. The Pr ions are seen to be weakly hybridized with the conduction electrons, and the magnetic ordering is orbitally driven, rather than spin driven. The theory[18] accounts qualitatively for the observed ordering in these materials.

Neutron elastic scattering experiments by Li *et al.*[16] were performed on $PrBa_2Cu_3O_{7-y}$ in order to determine details of the magnetic order. They found antiferromagnetic ordering for $T<T_N$, with the ordered moment along the c axis, similar to that found for $GdBa_2Cu_3O_{7-y}$.[19] The integrated intensity of one of the scattering lines, gives a magnetic moment in the ordered state of $0.74\pm0.08\mu_B$, consistent with a crystal-field-split Pr^{4+}, a ground-state doublet which would have a moment of the order of the observed moment, namely, $0.71\mu_B$. Along with the large ordering temperature, this suggests that f-electron hybridization effects may play a role in the magnetic ordering of $PrBa_2Cu_3O_{7-y}$. Although the neutron scattering results verify the presence of long-range magnetic ordering for $T<17$ K, they do not explain the increasing susceptibility for $T<17$ K, nor do they shed any light on the high value of T_N. Finally we note that it is possible that ordering along directions other than the c axis may exist but perhaps was missed in the neutron scattering experiments due to the low Pr moment.

A satisfactory explanation of the magnetic ordering of $PrBa_2Cu_3O_{7-y}$ must account for the semiconducting environment in which the ordering takes place. This implies that a superexchange mechanism involving hybridization of f electrons with the electrons associated with the Cu-O sheets, i.e., those responsible for the superconductivity of the undoped material, must be invoked to explain Pr-moment coupling. Discussions of the measurements described further reinforce the contention that there is strong hybridization and valence mixing in this system.

IV. SUPERCONDUCTIVITY AND MAGNETISM IN $(Y_{1-x}Pr_x)Ba_2Cu_3O_{7-y}$

Recalling the data of Fig. 1, which showed the smooth transition from superconductivity to ordered magnetism in $Y_{1-x}Pr_xBa_2Cu_3O_{7-y}$ from $x=0$ to 1.0, we show in Fig. 8(a) the electrical resistivity versus temperature, $\rho(T)$ for six samples covering a wide range of Pr concentration. Note there are 2 orders of magnitude difference in the vertical scales of 8(a) and 8(b). These data are similar to those of Ref. 5. The electrical resistivity for $PrBa_2Cu_3O_{7-y}$ is difficult to measure at low temperatures, but it appears to be around 10^7 Ω cm at 4.2 K, and there is negative magnetoresistivity at low temperatures. All four samples in Fig. 8(b) show superconductivity, and those near the critical concentration for suppression of superconductivity show small rises in $\rho(T)$ near T_c. Fits to $\rho(T)$ for the semiconducting samples did not yield

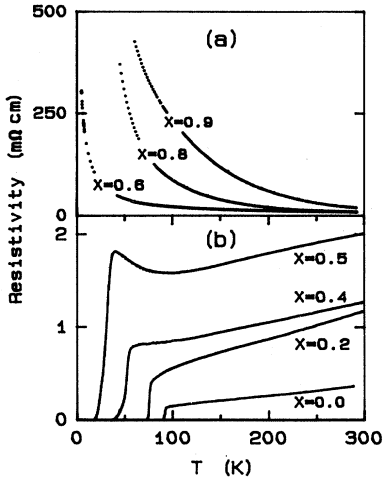

FIG. 8. Resistivity vs temperature for $Y_{1-x}Pr_xBa_2Cu_3O_{7-y}$ with $y \approx 0.1$.

simple single gap characteristics [$\ln\rho(T) \sim T^{-1}$] or variable range hopping characteristics [$\ln\rho(T) \sim T^{-1/4}$ or $\ln\rho(T) \sim T^{1/2}$]. The drastic increases in the electrical resistivity accompanying the transition from superconductivity to normal behavior of $(Y_{1-x}Pr_x)Ba_2Cu_3O_{7-y}$ is also characteristic of other systems, for example, $YBa_2(Cu_{1-x}Zn_x)_3O_{7-y}$,[20] and for oxygen-depleted $YBa_2Cu_3O_{7-y}$.[11,21] In order to illustrate this transition we show the resistivity at 100 K for several $(Y_{1-x}Pr_x)Ba_2Cu_3O_{7-y}$ samples in Fig. 9. Clearly the semiconducting behavior accompanies the destruction of the superconducting phase. In the $YBa_2(Cu,Zn)_3O_7$ system, there was clear evidence of d-electron localization accompanying the dramatic increase of $\rho(T)$ versus Zn concentrations which occurred at that Zn concentration needed to depress $T_c \rightarrow 0$. The most dramatic evidence for the localization of d electrons came from electron spin resonance (ESR) studies which displayed rapid growth in the intensity of the ESR resonance for Zn concentrations greater than that necessary to depress $T_c \rightarrow 0$. Other evidence of localization was also evident in $C(T)$ and $\chi(T)$ data. The localization occurring in the $YBa_2(Cu,Zn)_3O_7$ system was attributed to a disruption of the Cu($3d$)-O($2p$) hybridization within the two-dimensional bands associated with the Cu-O planes. For $Y_{1-x}Pr_xBa_2Cu_3O_{7-y}$, there is no supportive evidence in $\chi(T)$ or ESR (Ref. 22) for a corresponding localization for $x > x_{cr}$, where x_{cr} is that concentration which depresses $T_c \rightarrow 0$. There is no ESR response seen for any x in $Y_{1-x}Pr_xBa_2Cu_3O_{7-y}$ with $y = 0.1$.[22] Such data also indicates that these samples are quite clean with respect to second phases such as $BaCuO_{2+x}$ and Y_2CuBaO_5, which have been shown to produce large ESR responses.[23] On the other hand, the absence of ESR response does not exclude localization.

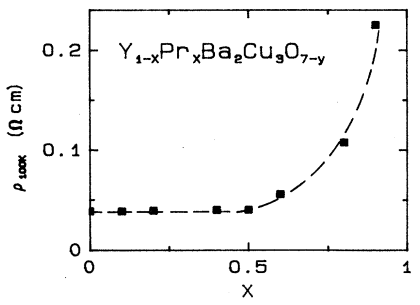

FIG. 9. Resistivity of $Y_{1-x}Pr_xBa_2Cu_3O_{7-y}$ at $T = 100$ K vs Pr-concentration x.

In Fig. 10 we show the specific heat at low temperature ($T < 10$ K), displayed in the customary C/T versus T^2 manner in order to emphasize the low-temperature electronic contribution to $C(T)$. All three specimens are superconducting, with $T_c = 90$, 75, and 50 K, for the $x = 0.0$, 0.2, and 0.4 samples, respectively. In the lower part of the figure, a slight enhancement of $C(T)$ with magnetic field is evident for the $x = 0.2$ sample. For all the data of Fig. 10, the superconducting entropy is expected to be removed since $T \ll T_c$, so that the normal contribution to the electronic heat capacity should dominate for $T < 10$ K. The data for the $x = 0.2$ and 0.4 samples are reminiscent of those for heavy-fermion systems,[24] namely, high values of C/T, which measures the electronic density of states at the Fermi surface. The value of C/T for the $x = 0.4$ sample reaches 200 mJ/mol K^2, which is in the "heavy-fermion" range. Perhaps this represents increased hybridization of the Pr ions with the conduction electrons near the critical concentration for superconductivity suppression, as suggested by Cooper.[18] Although there are upturns in C/T (as one lowers T) for most materials, the data for the $x = 0.4$ sample is particularly interesting due to the low-temperature downturn in C/T. This may be evidence for spin-wave-type excitations at low temperatures, indicating incipient magnetic ordering for $T < 3$ K in the super-

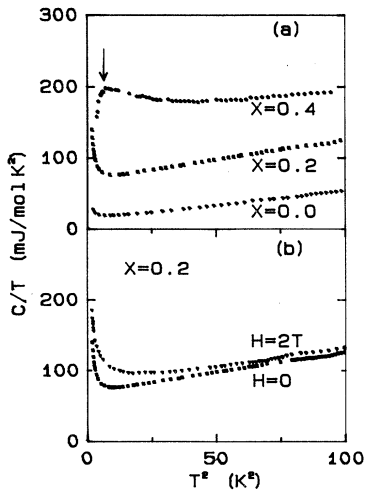

FIG. 10. The specific heat divided by temperature vs the temperature squared for $Y_{1-x}Pr_xBa_2Cu_3O_{7-y}$ with $y \approx 0.1$ and $0 \leq x \leq 0.4$.

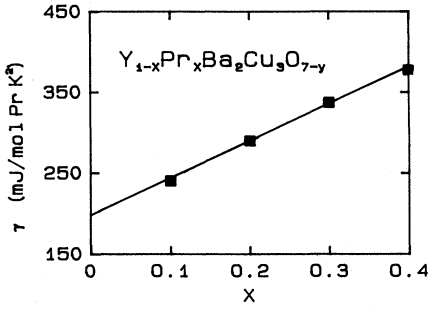

FIG. 11. The electronic specific heat coefficient per Pr ion vs Pr concentration for $Y_{1-x}Pr_xBa_2Cu_3O_{7-y}$ with $y=0.1$.

conducting state ($T_c=50$ K for this sample). The temperature where $C(T)/T$ versus T^2 begins to decrease is indicated by an arrow in Fig. 10 and the open circles in Fig. 1. These temperatures lie close to the extrapolated T_N versus x data obtained from $d\chi/dT$ versus T for samples in the nonsuperconducting regime. The extrapolated electronic heat-capacity coefficient γ per mole Pr versus x is shown in Fig. 11. They were obtained by subtracting the $x=0$ data and fitting C/T to $\gamma+\beta T^2$ in the temperature range between 5 and 10 K. A clear trend to larger γ and, hence, higher correlated states is seen with increasing Pr concentration, perhaps reflecting increased localized moment-conduction electron hybridization at low temperatures.

The magnetic ordering temperatures as a function of x for the Pr-rich samples of $(Y_{1-x}Pr_x)Ba_2Cu_3O_{7-y}$ were

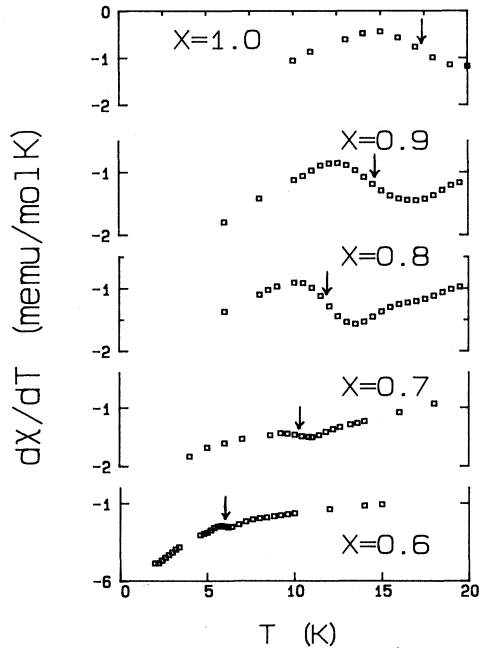

FIG. 12. The temperature derivative of the magnetic susceptibility vs temperature for $Y_{1-x}Pr_xBa_2Cu_3O_{7-y}$ with $y=0.1$ and $0.6\leq x\leq 1.0$. The Néel temperatures, T_N are indicated by arrows.

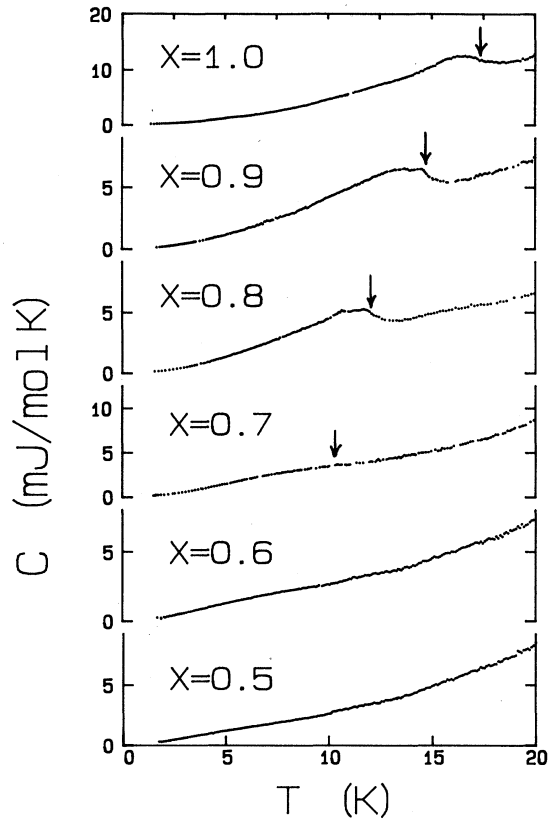

FIG. 13. The specific heat vs temperature for $Y_{1-x}Pr_xBa_2Cu_3O_{7-y}$ with $y=0.1$ and $0.5\leq x\leq 1.0$. The Néel temperatures T_N are indicated by arrows.

best determined by the temperature derivative of the magnetic susceptibility. This is seen in Fig. 12, where the arrows indicate the position of the steepest negative slope. In Fig. 13 we show $C(T)$ versus T up to 20 K for several high-Pr-content samples. The magnetic ordering temperatures are indicated by arrows in both Figs. 12 and 13. For $PrBa_2Cu_3O_{7-y}$, T_N obtained from $d\chi/dT$ and $C(T)$ agree with the temperature at which the ordered moment goes to zero.[16] As seen in Fig. 14, T_N decreases

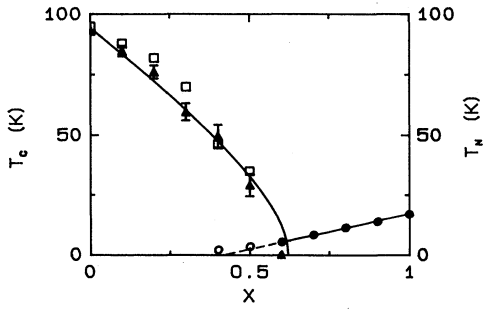

FIG. 14. Superconducting transition temperature T_c and Néel temperature T_N vs x for $Y_{1-x}Pr_xBa_2Cu_3O_{7-y}$ with $y\approx 0.1$. [▲$-T_c$ obtained from $\rho(T)$, □$-T_c$ obtained for $\chi(T)$, ●$-T_N$ obtained for $d\chi/dT$ and $C(T)$, 0$-T_N^*$ obtained for C/T vs T^2.]

linearly with decreasing Y concentration in the range $1 \geq x \geq 0.6$. An extrapolation of T_N versus x yields a critical concentration to depress $T_N \rightarrow 0$ of $x \approx 0.4$ and a possible region of coexistence of superconductivity and magnetic order. However, one must be concerned with the possibility that the two phenomena are occurring in different physical parts of the sample. Although we have no microscopic evidence bearing on this issue, indirect evidence from the concentration dependence of the lattice constants, specific heat, T_N, and T_c suggest that both are occurring throughout the bulk of the sample. $d\chi/dT$ versus T provided the clearest definition of $T_N(x)$ but for $x < 0.6$ superconducting diamagnetic shielding interferes with such a measurement. Returning to Fig. 10, $C(T)/T$ versus T^2 for $x < 0.4$ displays a pronounced upswing as $T^2 \rightarrow 0$. For $x = 0.4$ and 0.5 this upswing is suppressed indicating the onset of partial magnetic ordering or correlations (spin-wave-type excitations). Shown in Fig. 14 as open circles are T_N^* for $x = 0.4$ and 0.5, where T_N^* corresponds to the temperature where $C(T)/T$ versus T^2 has an apparent downturn. It is not clear whether these transition temperatures truly represent a long-range ordering temperature. The T_N^* deviate from a linear extrapolation of T_N versus x for $x > 0.6$. If T_N^* approximately represents T_N this deviation could reflect the interplay between superconductivity and magnetism. Changes in the effective exchange interaction within the superconducting state are expected, due to a change in the conduction-electron-spin susceptibility. Such effects have been observed in conventional superconducting systems doped with rare-earth impurities.[25] Further work is required to more clearly establish the nature of the possible coexistence region and changes in both the magnetic and superconducting phase boundaries due to interplay between these two ordered states.

Continuing with the magnetic and superconducting properties of some of the $(Y_{1-x}Pr_x)Ba_2Cu_3O_{7-y}$ samples, we show in Fig. 15 the inverse of the high-temperature magnetic susceptibility above T_c for two of the superconducting samples. Also shown is the field-cooled Meissner effect magnetization for three samples (inset of Fig. 15). The superconducting transition temperatures as determined from the onset of a diamagnetic response are also shown in Fig. 14 along with T_c determined from $\rho(T)$ data. Both measurements provide a consistent determination of the normal-superconducting state phase boundary. In Fig. 14, the solid line tracing out the normal-superconducting phase boundary is a fit to the classic Abrikosov-Gorkov pair-breaking theory,

$$\ln(T_c/T_{c0}) = \Psi(\tfrac{1}{2}) - \Psi(\tfrac{1}{2} + e^{-\gamma} x T_{c0}/4x_{cr}T_c) ,$$

where x_{cr} is the critical concentration and Ψ is the digamma function. The critical concentration $x_{cr} = 0.62$ is uniquely related to the initial slope of T_c versus x, i.e.,

$$dT_c/dx = -\pi^2 e^{-\gamma} T_{c0}/8x_{cr} ,$$

where γ is Euler's constant. The agreement between the measured T_c versus x and the standard pair-breaking relationship is remarkable.[8,9] As illustrated in the inset of Fig. 16, which also shows the inverse susceptibility for the $x = 0.4$ and 1.0 samples, the effective high-temperature paramagnetic moment is essentially independent of Pr content over the entire series. The value lies close to the effective moment for Pr^{4+}, namely $2.54\mu_B$, and is in good agreement with Dalichaouch *et al.*[3]

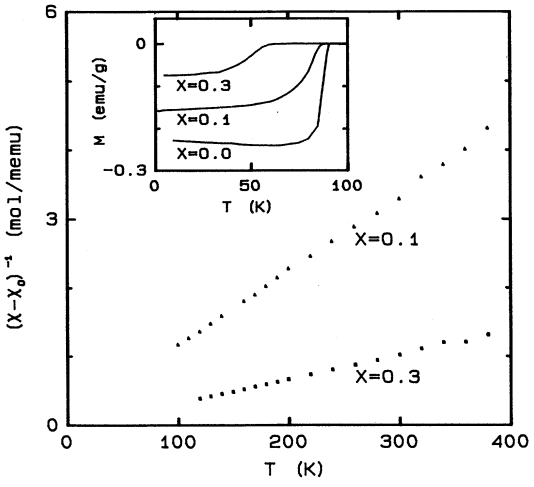

FIG. 15. $(\chi - \chi_0)^{-1}$ vs temperature for dilute $Y_{1-x}Pr_xBa_2Cu_3O_{7-y}$ samples. Here the constant χ_0 is determined from a fit to $\chi = \chi_0 + C/(T + T^*)$. Shown in the inset is the magnetization versus temperature for samples cooled in a field of 75 G.

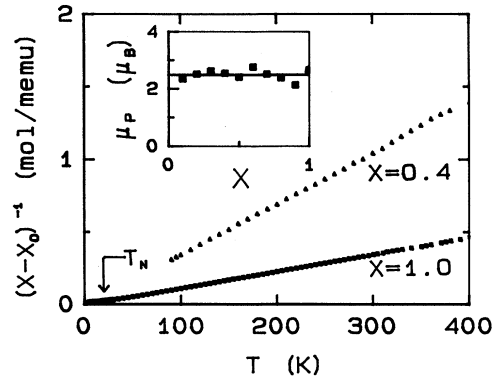

FIG. 16. $(\chi - \chi_0)^{-1}$ vs temperature for pure $PrBa_2Cu_3O_{7-y}$ and $Y_{0.6}Pr_{0.4}Ba_2Cu_3O_{7-y}$. The Néel temperature determined from $d\chi/dT$ is indicated as T_N. The inset shows the paramagnetic moment for the entire series $0 \leq x \leq 1$.

V. CONCLUSIONS

In this paper we present an extensive study of the magnetic, thermal, and superconducting properties of $(Y_{1-x}Pr_x)Ba_2Cu_3O_7$. The endpoints of the alloy series, namely, the compounds Y-Ba-Cu-O and Pr-Ba-Cu-O, are a high-temperature superconductor and a magnetic semiconductor, respectively. Alloying reduces both the superconductivity and the magnetic order, and gives rise to a region $(0.4 < x < 0.6)$ where antiferromagnetism and su-

perconductivity are likely to coexist. We show the corresponding phase diagram in Fig. 1.

The most remarkable feature (noted previously in Ref. 3) is that Pr substituted into Y-Ba-Cu-O behaves very differently from almost all other rare-earth ions, which do not depress the superconductivity. From the fact that T_c versus x closely follows an Abrikosov-Gorkov pair-breaking curve with $x_{cr} \approx 0.62$, one would conclude that the magnetic moment of the Pr ions interacts with the conduction electrons responsible for the superconductivity,[8,9] unlike the other rare-earth ions (except Ce and Tb, which apparently do not form in the same structure). Furthermore, the relatively high Néel temperature of Pr-Ba-Cu-O ($T_N = 17$ K as compared to 2.2 K for Gd-Ba-Cu-O, i.e., two orders-of-magnitude larger than expected from a de Gennes scaling) strongly suggests that the interaction mechanism between Pr ions is different (and considerably stronger) than the one between other rare-earth ions. The lack of field-dependence of T_N for Pr-Ba-Cu-O (shown and compared to Gd-Ba-Cu-O in Fig. 6) and the continuing increase of the susceptibility when the temperature is lowered below T_N are other indications of the distinct properties of the Pr ions. On the other hand, the same simple antiferromagnetic order as for Gd-Ba-Cu-O was observed via neutron scattering.

These properties cannot be explained assuming trivalent Pr ions. Instead they suggest that the Pr ions have some mixed-valent character, which accounts for the exchange coupling with the conduction electrons in the adjacent Cu-O planes. The high-temperature magnetic moment of the Pr ions as obtained from the Curie constant of the susceptibility is independent of the Pr concentration and close to that of the tetravalent ion. The superconducting to normal transition as a function of Pr content is accompanied by a transition into a semiconducting phase, similar to oxygen depleted Y-Ba-Cu-O and Zn-doped Y-Ba-Cu-O. In the latter two cases the metal-insulator transition is explained by the filling of d holes and localization of states due to disorder in the Cu-O planes. The analogy suggests that Pr is close to tetravalent, so that the additional electron (Pr^{4+} versus Y^{3+}) reduces the number of available d holes in addition to introducing some disorder in the planes. This interpretation is however not supported by spectroscopic observations.[26] Note that Pr^{4+} has the same electronic configuration as Ce^{3+}. In a strong crystal field of orthorhombic symmetry the ground state is expected to be a doublet, while for Pr^{3+} it would be a ground singlet. The antiferromagnetic order and the entropy removal at the transition (about ln2 per Pr ion) strongly support the Pr^{4+} hypothesis. The large γ values, the AG curve followed by T_c and the large Néel temperature can then be understood with some valence admixing from the Pr^{3+} configuration.

As already discussed,[9] the relative initial T_c depression rates, i.e., dT_c/dx, are very different for Pr (115 K per Pr fraction) as compared to Zn (1000 K per Zn-fraction) substitutions. In neither case can the T_c depression be attributed just to a filling of d holes, but at least in the case of $YBa_2(Cu,Zn)_3O_{7-y}$ a localization of states within the Cu-O planes must be invoked. Evidence for such a localization is the ESR signal, which is almost absent in the superconducting-metallic phase and shows a rapid rise for Zn concentrations larger than the critical. An ESR bulk response was not observed in $(Y,Pr)Ba_2Cu_3O_{7-y}$,[22] probably implying a lesser degree of localization. This is consistent with the superconductivity being depressed by magnetic moments (AG curve). Another difference worth pointing out[9] is the curvature of T_c versus x for the two systems: while this curvature is negative for $(Y,Pr)Ba_2Cu_3O_{7-y}$, it is positive for $YBa_2(Cu,Zn)_3O_{7-y}$.

ACKNOWLEDGMENTS

We are pleased to acknowledge helpful discussions with S. Foner of the Francis Bitter National Laboratory, where most of the magnetic measurements were performed. The Temple University effort was supported by the National Science Foundation (NSF) Grant No. DMR8802401; the Tufts University work was supported by NSF Grant No. DMR8502077; and P.S. acknowledges the support by the U.S. Department of Energy (DOE) under Grant No. DE-FG02-87ER45333.

[1] Z. Fisk, J. D. Thompson, E. Zirngiebl, J. L. Smith, and S.-W. Cheong, Solid State Commun. **62**, 743 (1987); P. Hor, R. L. Meng, Y. Qu. Wang, L. Gao, Z. J. Huang, J. Bechtold, K. Forster, and C. W. Chu, Phys. Rev. Lett. **58**, 1891 (1987).

[2] M. B. Maple, L. E. Delong, and B. C. Sales, in *Handbook on the Physics and Chemistry of the Rare Earths,* edited by K. A. Gschneidner, Jr. and L. Eyring (North-Holland, Amsterdam, 1978), Vol. 1, p. 797.

[3] L. Soderholm, K. Zhang, D. G. Hinks, M. A. Beno, J. D. Jorgensen, C. U. Segre, and I. K. Schuller, Nature **328**, 604 (1987); J. K. Liang, X. T. Xu, S. S. Xie, G. H. Rao, X. Y. Shao, and Z. G. Duan, Z. Phys. B **69**, 137 (1987); Y. Dalichaouch, M. S. Torikachvili, E. A. Early, B. W. Lee, C. L. Seaman, K. N. Yang, H. Zhou, and M. P. Maple, Solid State Commun. **65**, 1001 (1988).

[4] A. Kebede, C.-S. Jee, D. Nichols, M. V. Kuric, J. E. Crow, R. P. Guertin, T. Mihalisin, G. H. Myer, I. Perez, R. E. Salomon, and P. Schlottmann, J. Magn. Magn. Mater. **76+77**, 619 (1988).

[5] M. B. Maple, Y. Dalichaouch, E. A. Early, B. W. Lee, J. T. Markert, M. W. McElfresh, J. J. Neumeier, C. L. Seaman, M. S. Torikachvili, K. N. Yang, and H. Zhou, *High T_c Superconductors,* edited by H. W. Weber (Plenum, New York, 1988), p. 29; M. B. Maple, Y. Dalichaouch, E. A. Early, B. W. Lee, J. T. Markert, J. J. Neumeier, C. L. Seaman, K. N. Yang, and H. Zhou, Physica C **153-5**, 858 (1988).

[6] K. N. Yang, B. W. Lee, M. B. Maple, and S. S. Laderman, Appl. Phys. **A46**, 229 (1988).

[7] See, for example, *Crystalline Electric Field Effects in f-Electron Magnetism,* edited by R. P. Guertin, W. Suski, and Z. Zol-

nierek (Plenum, New York, 1982), pp. 1–99.
[8]C.-S. Jee, A. Kebede, T. Yuen, S. H. Bloom, M. V. Kuric, J. E. Crow, R. P. Guertin, T. Mihalisin, G. H. Myer, and P. Schlottmann, J. Magn. Magn. Mater. **76+77**, 617 (1988).
[9]C.-S. Jee, A. Kebede, D. Nichols, J. E. Crow, T. Mihalisin, G. H. Myer, I. Perez, R. E. Salomon, and P. Schlottmann, Solid State Commun. **69**, 379 (1989).
[10]W. Wong-Ng, H. F. McMurdie, B. Paretzkin, C. R. Hubbard, A. L. Dragoo, and J. M. Stewart, Powder Diffract. **2**, 116 (1987).
[11]J. M. Tarascon, W. R. McKinnon, L. H. Greene, G. W. Hull, and E. M. Vogel, Phys. Rev. B **36**, 226 (1987).
[12]R. D. Shannon and C. T. Prewitt, Acta Crystallogr. B **25**, 925 (1969).
[13]J. W. Lynn (private communication).
[14]D. E. Farrell, B. S. Chandrasekhar, M. R. DeGuire, M. M. Fang, V. G. Kogan, J. R. Clem, and D. K. Finnemore, Phys. Rev. B **36**, 4025 (1987).
[15]S. H. Bloom, M. V. Kuric, R. P. Guertin, C.-S. Jee, D. Nichols, E. Kaczanowicz, J. E. Crow, G. Myer, and R. E. Salomon, J. Magn. Magn. Mater. **68**, L135 (1987).
[16]W.-H. Li, J. W. Lynn, S. Skanthakumar, T. W. Clinton, A. Kebede, C.-S. Jee, J. E. Crow, and T. Mihalisin, Phys. Rev. B (to be published).
[17]J. C. Ho, P. H. Hor, R. L. Meng, C. W. Chu, and C. Y. Huang, Solid State Commun. **63**, 711 (1987); J. O. Willis, Z. Fisk, J. D. Thompson, S. W. Cheong, R. M. Aikin, J. L. Smith, and E. Zirngiebl, J. Magn. Magn. Mater. **67**, L139 (1987).
[18]B. R. Cooper, in *Proceedings of the High T_c Superconductors: Magnetic Interactions,* edited by L. H. Bennett, Y. Flom, and C. G. Vezzolli (World Scientific, Singapore, 1989), p. 7.
[19]D. Mck. Paul, H. A. Mook, A. W. Hewat, B. C. Sales, L. A. Boatner, J. R. Thompson, and M. Mostoller, Phys. Rev. B **37**, 2341 (1988).
[20]C.-S. Jee, D. Nichols, A. Kebede, S. Rahman, J. E. Crow, A. M. Ponte Goncalves, T. Mihalisin, G. H. Myer, I. Perez, R. E. Salomon, P. Schlottmann, S. H. Bloom, M. V. Kuric, Y. S. Yao, and R. P. Guertin, J. Superconductivity **1**, 63 (1988).
[21]R. J. Cava, B. Batlogg, C. H. Chen, E. A. Rietman, S. M. Zahurak, and D. Werder, Phys. Rev. B **36**, 5719 (1987).
[22]S. Tyagi (private communication).
[23]D. C. Vier, S. B. Oseroff, C. T. Salling, J. F. Smyth, S. Shultz, Y. Dalichaouch, B. W. Lee, M. B. Maple, Z. Fisk, and J. D. Thompson, Phys. Rev. B **36**, 8888 (1987).
[24]G. R. Stewart, Rev. Mod. Phys. **56**, 755 (1984).
[25]M. B. Maple, in *Magnetism,* edited by H. Suhl (Academic, New York, 1973), Vol. V, p. 289; Ø. Fisher and M. Peter, *ibid.*, p. 327.
[26]S. Horn (private communication).